

THE OFFICIAL MAGAZINE OF THE OCEANOGRAPHY SOCIETY

Oceanography

CITATION

Rudnick, D.L., S. Jan, L. Centurioni, C.M. Lee, R.-C. Lien, J. Wang, D.-K. Lee, R.-S. Tseng, Y.Y. Kim, and C.-S. Chern. 2011. Seasonal and mesoscale variability of the Kuroshio near its origin. *Oceanography* 24(4):52–63, <http://dx.doi.org/10.5670/oceanog.2011.94>.

DOI

<http://dx.doi.org/10.5670/oceanog.2011.94>

COPYRIGHT

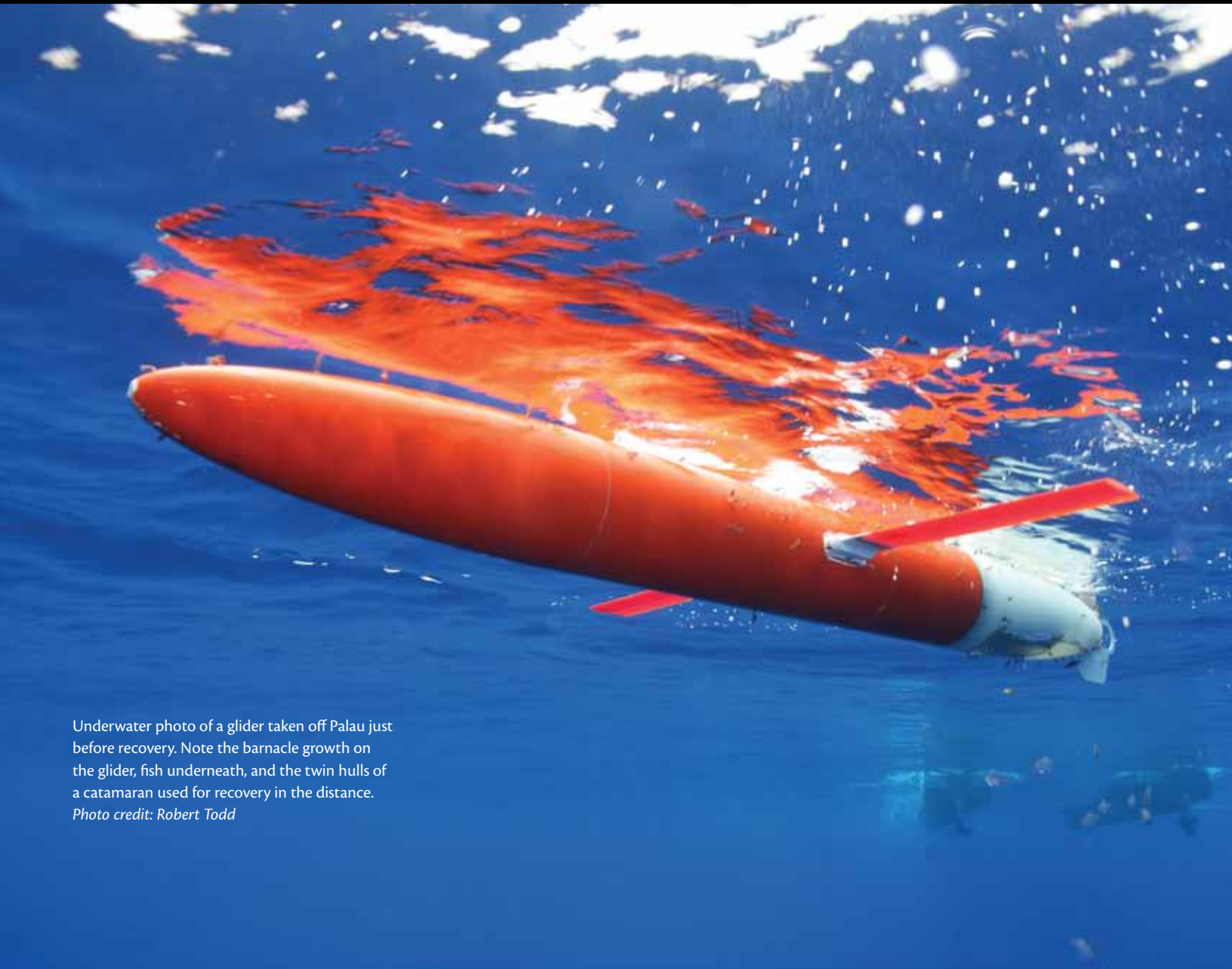
This article has been published in *Oceanography*, Volume 24, Number 4, a quarterly journal of The Oceanography Society. Copyright 2011 by The Oceanography Society. All rights reserved.

USAGE

Permission is granted to copy this article for use in teaching and research. Republication, systematic reproduction, or collective redistribution of any portion of this article by photocopy machine, reposting, or other means is permitted only with the approval of The Oceanography Society. Send all correspondence to: info@tos.org or The Oceanography Society, PO Box 1931, Rockville, MD 20849-1931, USA.

Seasonal and Mesoscale Variability of the Kuroshio Near Its Origin

BY DANIEL L. RUDNICK, SEN JAN, LUCA CENTURIONI, CRAIG M. LEE, REN-CHIEH LIEN,
JOE WANG, DONG-KYU LEE, RUO-SHAN TSENG, YOO YIN KIM, AND CHING-SHENG CHERN



Underwater photo of a glider taken off Palau just before recovery. Note the barnacle growth on the glider, fish underneath, and the twin hulls of a catamaran used for recovery in the distance.
Photo credit: Robert Todd



ABSTRACT. The Kuroshio is the most important current in the North Pacific. Here, we present historical data and recent observations of the Kuroshio off the coasts of Taiwan and the Philippine Archipelago, with a focus on its origins. Seasonal climatologies from shipboard hydrographic and velocity measurements, and from surface drifters, demonstrate changes in the Kuroshio caused by the monsoon. In particular, seasonal monsoon forcing affects the degree of penetration of the Kuroshio through Luzon Strait. Data from surface drifters and underwater gliders describe its mesoscale variability. Velocities derived from drifters make clear the mesoscale variability associated with the Subtropical Countercurrent east of the Kuroshio. Underwater gliders document mesoscale structure prominent in salinity extrema associated with water masses. The evolution of these water masses as they progress northward near the Kuroshio indicates strong mixing in the region.

INTRODUCTION

Three major currents dominate the general circulation in the western Pacific offshore of Taiwan and the Philippines (Figure 1): the North Equatorial Current (NEC) flows westward, runs into the Philippine coast, and bifurcates into the northward-flowing Kuroshio and the southward-flowing Mindanao Current. As the terminus of the NEC, and the origin of the Kuroshio and Mindanao Current, this bifurcation region is globally important. Of these three currents, the Kuroshio has probably received the most study through observation, theory, and modeling. Here, we review some of this work and present new findings, with a focus on variability.

The Kuroshio starts as a relatively poorly defined current flowing from the bifurcation region (Figure 1). The current flows northward to the northern tip of Luzon Island, where it veers westward through Luzon Strait into the South China Sea (SCS). The Kuroshio generally does not penetrate very far into the SCS, but penetrating incursions happen occasionally. The Kuroshio becomes well established as it flows northeastward out of Luzon Strait along the east coast of Taiwan. By the time the

Kuroshio passes between Taiwan and the Ryukyu Islands, it is a strong, coherent current with a mean transport of 21 Sv ($1 \text{ Sv} = 10^6 \text{ m}^3 \text{ s}^{-1}$) (Johns et al., 2001).

The NEC supplies the western boundary with two distinct water masses marked by salinity extrema. North Pacific Tropical Water (NPTW) is marked by high salinity near 200 m depth, while North Pacific Intermediate Water (NPIW) is well known as a salinity minimum near 500 m depth. On the basis of chlorofluorocarbon observations, Fine et al. (1994) conclude that NPTW was in contact with the atmosphere less than three years before reaching the western boundary, while NPIW is less than 20 years old. As the water proceeds northward in the Kuroshio, the modification of these water masses is evident.

The Kuroshio's origin is marked by strong mesoscale variability, so strong, in fact, that it can overwhelm the mean flow offshore of Luzon. The mesoscale variability is due to at least two sources: (1) the instability of the Kuroshio itself, and (2) westward-propagating eddies arriving at the western boundary. The eastward-flowing Subtropical Countercurrent (STCC) is a region of

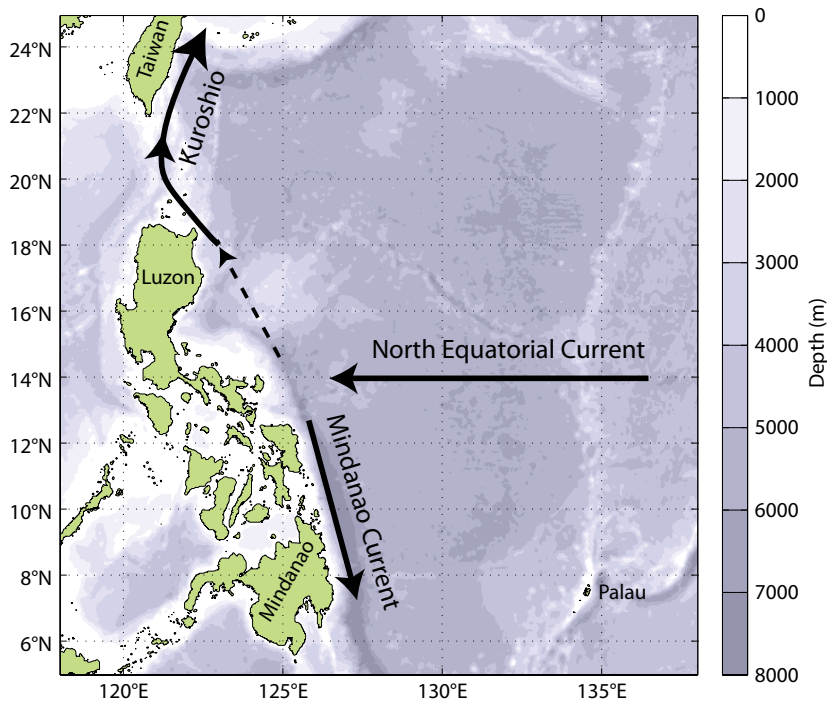


Figure 1. Schematic diagram of currents in the western Pacific off Taiwan and the Philippines. The North Equatorial Current (NEC) flows westward where it runs into the Philippine coast. The end of the NEC is the beginning of the northward Kuroshio and the southward Mindanao Current. The Kuroshio starts as a weak, unorganized current, and strengthens as it flows northward.

enhanced eddy activity centered at about 22°N (Qiu and Chen, 2010), presumably because of instability in the STCC. Qiu and Chen (2010) also find interannual changes in the strength of mesoscale variability related to vertical shear in both STCC and NEC. Regardless of

source, the region offshore of Taiwan has the second strongest mesoscale eddies in the entire North Pacific. The only region of stronger mesoscale variability in the North Pacific is the Kuroshio Extension offshore of Japan.

In the following, we summarize

Daniel L. Rudnick (drudnick@ucsd.edu) is Professor, Scripps Institution of Oceanography, La Jolla, CA, USA. **Sen Jan** is Associate Professor, Institute of Oceanography, National Taiwan University, Taipei, Taiwan. **Luca Centurioni** is Associate Project Scientist, Scripps Institution of Oceanography, La Jolla, CA, USA. **Craig M. Lee** is Principal Oceanographer, Applied Physics Laboratory, University of Washington, Seattle, WA, USA. **Ren-Chieh Lien** is Principal Oceanographer and Affiliate Professor, Applied Physics Laboratory, University of Washington, Seattle, WA, USA. **Joe Wang** is Professor, Institute of Oceanography, National Taiwan University, Taipei, Taiwan. **Dong-Kyu Lee** is Visiting Researcher, Scripps Institution of Oceanography, La Jolla, CA, USA. **Ruo-Shan Tseng** is Professor, Department of Marine Resources, National Sun Yat-sen University, Kaohsiung, Taiwan. **Yoo Yin Kim** is Senior Statistician, Scripps Institution of Oceanography, La Jolla, CA, USA. **Ching-Sheng Chern** is Professor, Institute of Oceanography, National Taiwan University, Taipei, Taiwan.

observations of variability in the Kuroshio and environs from recent observational campaigns. Shipboard acoustic Doppler current profiler (ADCP) and surface drifter data reveal variability in currents. Autonomous underwater gliders are used to quantify variations in hydrographic properties. A special focus is the passage of the Kuroshio across the mouth of Luzon Strait.

BOTTOM TOPOGRAPHY

The seafloor surrounding Taiwan has complicated topography (Figure 2). East of Taiwan, tectonic processes related to the flipping of subduction direction lead to great seafloor roughness. The Philippine Sea Plate subducts beneath the Eurasia Plate along the Ryukyu Trench. However, the Luzon Island Arc that belongs to the Philippine Sea Plate thrusts over the Eurasia continental margin (Liu et al., 1998). As a result, the topography east of Taiwan can be separated into three parts. The northern part is comprised of the northwest-southeast trending Okinawa Trough adjacent to the east-west trending Ryukyu Island Arc to the south. The middle part, roughly between 23°N and 24.5°N, is a 4,000–6,000 m deep basin called the Huatung Basin. Located south of the east-west trending Yaeyama Ridge, the Ryukyu Trench, with its maximal depth over 6,200 m, becomes shallow toward the west and loses its topographic character west of 122.5°E. In the southern part, the north-south trending Luzon Island Arc, which is the southern bound of the Huatung Basin, connects to the Coastal Mountain Range in south-eastern Taiwan. Green Island and Lanyu Island lie on the Luzon Island Arc off southeastern Taiwan.

WINDS

Winds measured by satellite remote sensing as well as at island weather stations off eastern Taiwan suggest that the East Asia monsoon dominates the change of wind, which is southwesterly to southerly in summer and northeasterly in winter. The winter northeasterly monsoon commences in mid-September, prevails from October to January, and weakens continuously thereafter. The summer southwesterly monsoon, prevailing from June to August, is much weaker than the winter monsoon, in particular, off southeastern Taiwan (Jan et al., 2006).

HISTORICAL HYDROGRAPHIC AND VELOCITY DATA

Since 1985, hydrography (temperature and salinity) and current velocity in the seas surrounding Taiwan have been continuously measured onboard R/Vs *Ocean Researcher 1*, *2*, and *3* under various scientific programs sponsored by the National Science Council (NSC) and the government agencies of Taiwan. More than 40,000 historical conductivity-temperature-depth (CTD) hydrographic casts from 1985 to 2010, and 3,500,000 current velocity profiles from 16 to 300 m depths measured by shipborne ADCP from 1991 to 2010 are stored in NSC's Ocean Data Bank operated by the Institute of Oceanography, National Taiwan University. The raw data have undergone quality control procedures following the standard recommended by the US National Oceanographic Data Center. In accordance with NSC policy, the archived data have been released to the public for purposes of scientific research, public infrastructure engineering, marine

search/rescue, and general education.

To update the climatology of the Kuroshio east of Taiwan after Liang et al. (2003), we analyze hydrography and current velocity data from the Ocean Data Bank collected before 2009. The shipboard ADCP ocean current velocity is blended with wind-driven and tidal components fluctuating at periods from a half-day to seasons. The barotropic tidal currents computed by a two-dimensional numerical tidal model described in Hu et al. (2010) are subtracted from the ADCP velocity data. The ocean is divided into $15' \times 15'$ grids;

both hydrographic and velocity data in each grid are interpolated to the center of the grid and then vertically interpolated at 10 m depth intervals. The corresponding climatological mean of hydrography and velocity are calculated at each grid when the data number is greater than three for hydrography and 30 for velocity data in each grid. It is natural to separate data collected in summer and winter because of the distinct monsoonal wind forcing. Accordingly, summer is defined as from May to September and winter from October to April.

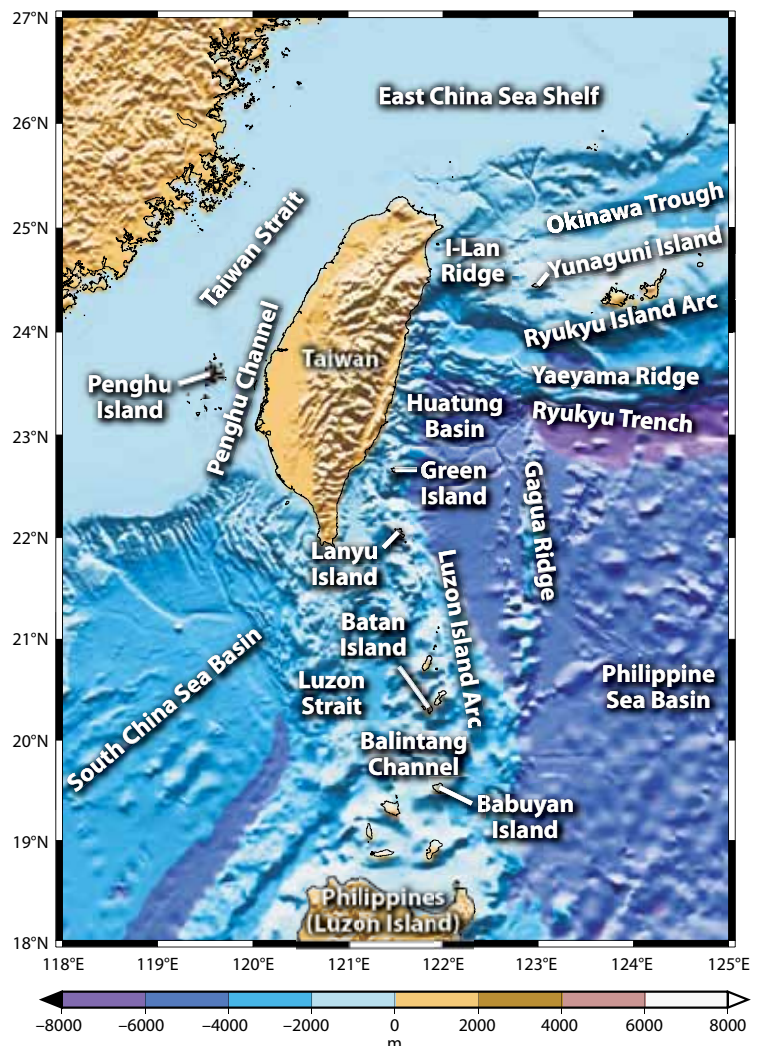


Figure 2. Bathymetric chart and topography in the seas surrounding Taiwan.

CLIMATOLOGY OF THE KUROSHIO EAST OF TAIWAN

Currents averaged over the upper 30 m in summer and winter show changes caused by monsoonal wind forcing (Figure 3). Beginning east of Luzon Island, the Kuroshio, with core velocity of about 1 m s^{-1} , flows northward across

Luzon Strait, hugs the east coast of Taiwan, and turns toward the north-east off northeastern Taiwan. Within Luzon Strait, the Kuroshio loops across the strait in summer (Figure 3a) but partly leaks into the northern South China Sea on its western flank in winter (Figure 3b). As the Kuroshio sweeps off

the southern tip of Taiwan, the main stream passes through the gap between Taiwan and Green Island. A core of strong flow likely from the Northwest Pacific subtropical gyre joins to the east flank of the Kuroshio east of Green Island. As the main Kuroshio and this eastern branch join, the Kuroshio narrows and strengthens in the short distance before it arrives at I-Lan Ridge. This section of Kuroshio is also called the “East Taiwan Current.” After passing over the Ryukyu Island Arc, the Kuroshio bumps into the East China Sea shelf break and turns northeastward, leaving the coast of Taiwan at roughly 25°N . According to the roughly 20-year statistics, the Kuroshio east of Taiwan is 100 km wide and 800–1,000 m deep, with the velocity core ranging from 1 to 1.5 m s^{-1} (Figure 3). The mean volume transport in the upper 300 m is 9.1 Sv at 22°N between Taiwan and Lanyu Island and is 15.7 Sv at 24°N between the coast and 123°E .

A recent survey using shipboard ADCP reveals the vertical structure of the Kuroshio as it enters Luzon Strait. In June 2010, during a neap tide, R/V *Revelle* collected several sections across the Kuroshio (Figure 3c). The

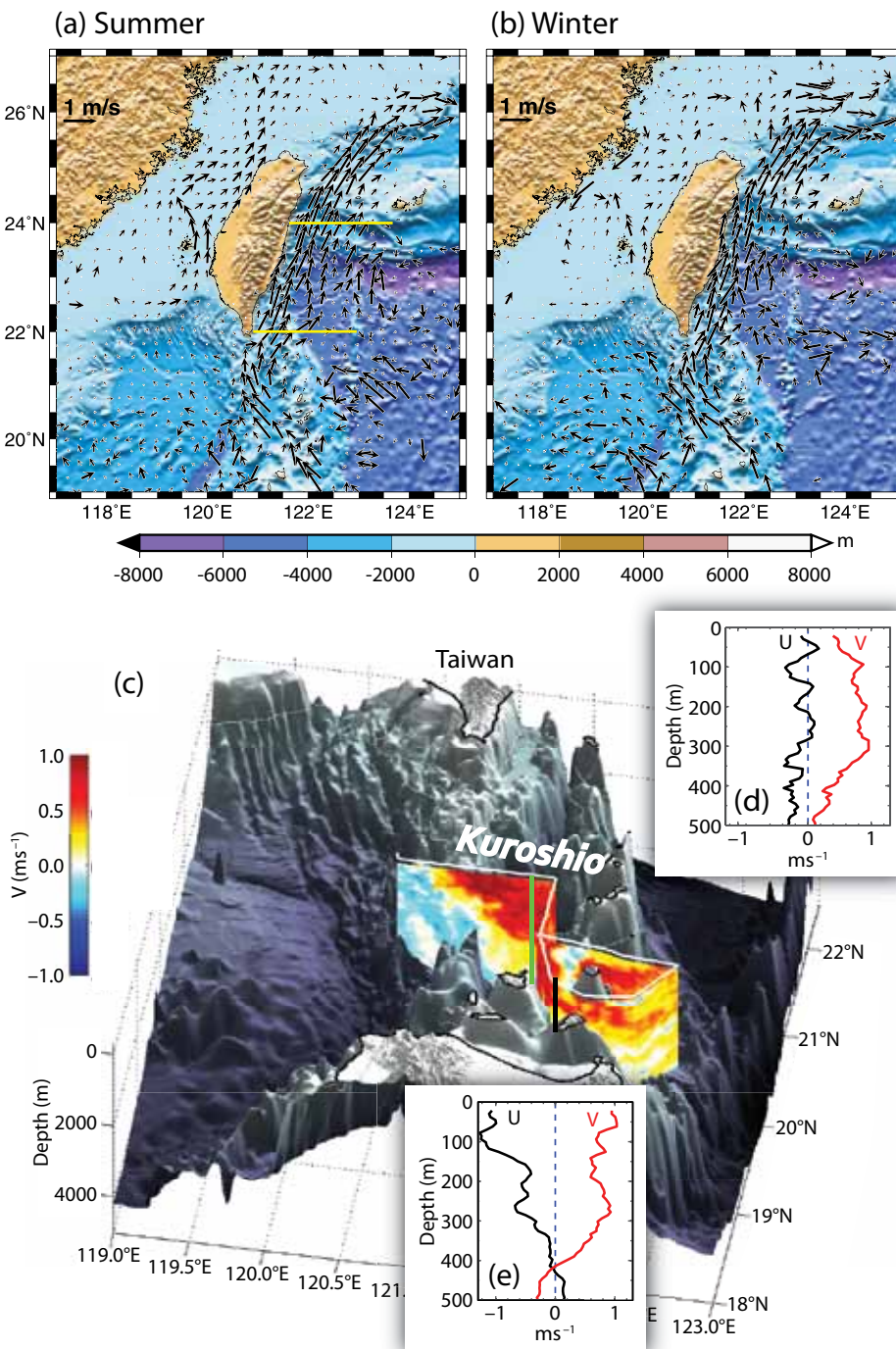


Figure 3. Climatological mean of shipboard acoustic Doppler current profiler (ADCP) velocity observations at 30 m depth in (a) summer and (b) winter, and sections of meridional velocity measurements from R/V *Revelle* shipboard ADCP in Luzon Strait in June 2010 (c). The depth scale of ADCP velocity contours in (c) is exaggerated by a factor of five in order to reveal the vertical structure of the Kuroshio (red shadings). The inserts (d) and (e) show the vertical profile of zonal and meridional velocity in the middle of Luzon Strait (green vertical line in panel c) and in Balintang Channel (black vertical line in panel c), respectively. Two yellow horizontal lines in (a) mark the zonal sections discussed in Figure 4.

section along 20.5°N in the middle of Luzon Strait shows that a strong northward Kuroshio exists between 120.75°E and the Luzon Island Arc, with a width of ~ 100 km. Along the axis of the Kuroshio (green vertical line in Figure 3c), the northward current is about 0.8 m s⁻¹ in the upper 300 m, decreasing nearly linearly to zero around 500 m depth (Figure 3d). The average zonal current in the upper 500 m is -0.13 m s⁻¹, much smaller than the average meridional current of 0.5 m s⁻¹. Within the Balintang Channel (black vertical line in Figure 3c), a strong westward current of 1–1.2 m s⁻¹ exists in the upper 100 m, and the northward current is similar to that in the middle of Luzon Strait (Figure 3e). The flow pattern is consistent with the climatological mean (Figure 3a,b).

Figure 4 shows sections of northward velocity, temperature, and salinity across the Kuroshio at 22°N and 24°N (two horizontal yellow lines in Figure 3a). The major velocity core is narrower but deeper at 22°N, and a weaker but visible velocity core is seen in the upper 100 m at 122.25°E. However, at 24°N, there is only one wider but shallower velocity core. A coastal countercurrent exists below 150–200 m depths on both sections. The isotherm tilt on the west flank of the Kuroshio is consistent with the geostrophic balance (Figure 4, middle panels). Isotherms level off below 700 m, indicating the vertical extent of the Kuroshio. The average temperature in the upper 50–100 m reaches 30°C in summer and decreases to 26°C in winter. The salinity west of the Kuroshio in the upper 50 m layer is lower (34–34.2) in summer than in winter (Figure 4, lower panels). This

water is the relatively fresh northern South China Sea water coming from the western Luzon Strait and attaching to the left side of the Kuroshio off southern-most Taiwan. A salinity maximum layer (NPTW) is seen between 150 to 250 m depths where the salinity is greater than 34.8 in both seasons. A salinity minimum (~ 34.2) layer (NPIW) is

seen from 500 to 650 m depth without distinct seasonal variation.

The core of the Kuroshio bends to the northeast following topography north of Taiwan. The surface expression of the Kuroshio is shifted landward in winter relative to summer (Figure 3). The strong winter northeast monsoon likely plays a role in this shift in Kuroshio position.

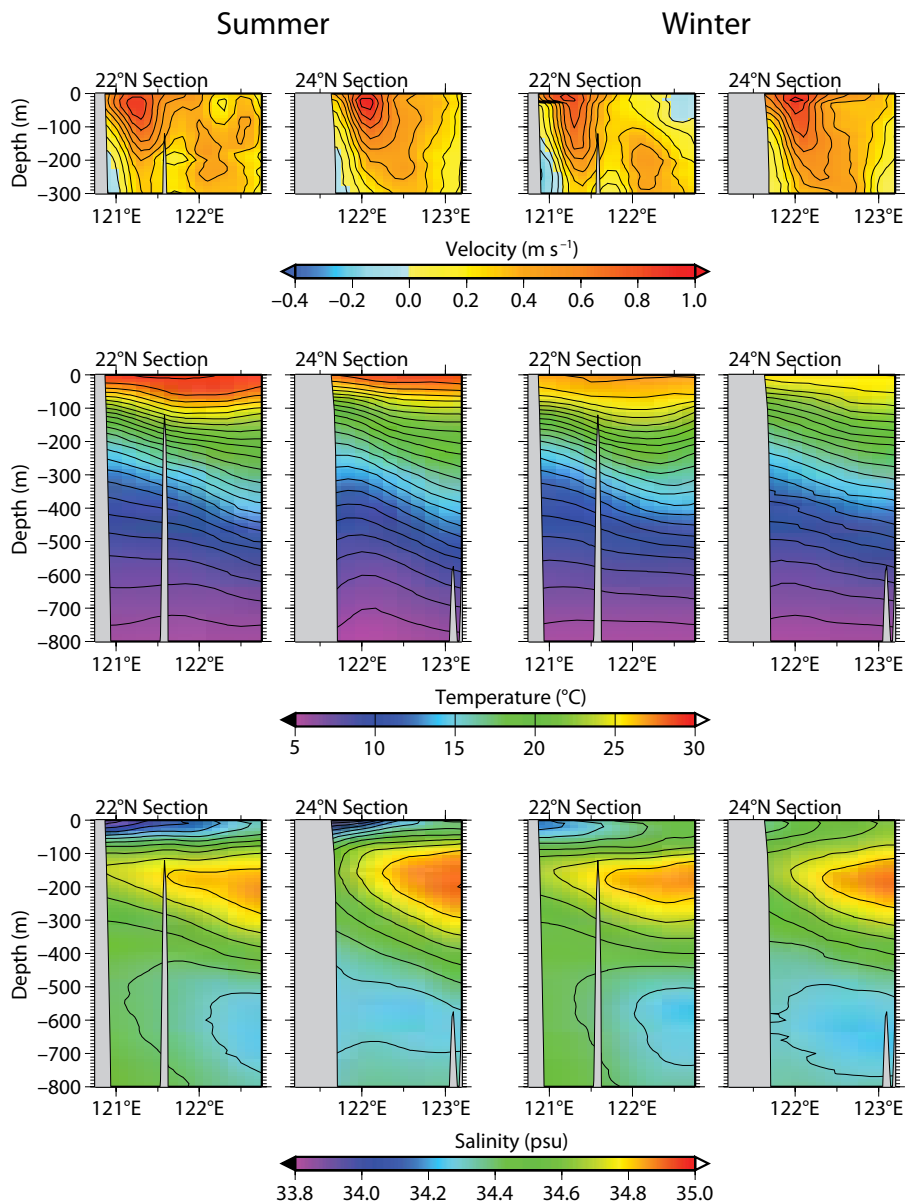


Figure 4. Zonal sections of climatological mean meridional velocity (top panels), temperature (middle panels), and salinity (bottom panels) variations along 22°N and 24°N, (two horizontal yellow lines in Figure 3a), in summer and winter. Contour interval is 0.1 m s⁻¹ for velocity, 1°C for temperature, and 0.1 psu for salinity.

Other mechanisms that may cause seasonal variations in the Kuroshio are changes in the NEC, fluctuations in volume transport through Taiwan Strait, and mesoscale eddies.

OBSERVATIONS FROM SURFACE DRIFTERS

In the past decade, the US Office of Naval Research (ONR) has sponsored several Lagrangian experiments in the seas around Taiwan: South China Sea (SCS), East China Sea, Philippine Sea, Japan East Sea, Taiwan Strait, and Luzon Strait. The main common goal of these Lagrangian programs was to improve understanding of the dynamical bases of the interactions of the Kuroshio with the seas around Taiwan by obtaining new observations of ocean currents at 15 m depth. Of particular interest was the seasonal variability of the Kuroshio in Luzon Strait, the seasonal circulation of the northern SCS and Taiwan Strait, the mesoscale variability east of Taiwan, and the intrusion of the Kuroshio onto the continental shelf of the southern East China Sea. Multiyear deployments of Surface Velocity Program (SVP) drifters

(Niiler, 2001) in Luzon Strait, in the northern SCS, and east of Taiwan permit construction of a time series. At the time of this writing, a line of drifters is being released monthly in the Philippine Sea (Table 1). During the last decade, a total of more than 600 SVP drifters have been deployed in the Northwest Pacific in support of ONR activities. Drifters were released mainly by Voluntary Observing Ships (VOS), with the exception of few deployments from joint US-Taiwan cruises in 2005, 2007, 2008, and 2009. VOS operated by the Hanjin Shipping Company, Hyundai, and the Taiwanese Coast Guard were central to the success of the programs. The US National Oceanic and Atmospheric Administration (NOAA)-funded Global Drifter Program also contributed significantly to the Northwest Pacific drifter array described here.

The near-surface currents measured by the Northwest Pacific SVP drifter array are markedly seasonal (Figure 5) and seemingly in phase with the monsoonal winds. From October through March, a period that includes the northeast monsoon, the Kuroshio

often enters the SCS through Luzon Strait, and is believed to provide an upper-ocean net westward mass transport from the Philippine Sea into the SCS (Centurioni et al., 2004, 2009). The cyclonic circulation of the northern SCS is intensified along the rim of the basin and appears to form a continuous current system that connects the swift Luzon Strait throughflow and the fast southward current off Vietnam (Centurioni et al., 2009). The currents in Taiwan Strait become progressively more southward as winter advances because the southward-moving cold and fresh East China Sea water modifies the summer mass distribution that maintains the northeastward flow from the SCS into the East China Sea (Jan et al., 2002). Interestingly, while a northward current is still present in Taiwan Strait in fall and early winter, none of the drifters that enter the SCS with the intruding Kuroshio reach Taiwan Strait through the Penghu Channel.

From April through September, a period that includes the southwest monsoon, the Kuroshio intrusion into the SCS disappears (Figure 5b),

Table 1. Summary of drifters deployed and anticipated deployments in the seas around Taiwan for the period from October 2003 through July 2012.

Region	Time span and months	Periodicity	Number of drifters released
Northern South China Sea, Luzon Strait, and Taiwan Strait	2003–2006, October through January	Weekly, five drifters per week drogued at 15 m depth and 75 drifters drogued at 150 m depth in 2006	255
Northern South China Sea	2005 and 2007, April and May	One deployment per year, 25 drifters in 2007, 10 drifters in 2007	35
North Pacific, east of southern Taiwan and northeast of Taiwan	April 2007 to September 2009, continuous	Two drifters per week up to January 2009, then one drifter per week; 122 drifters in July and August 2009	234
Philippine Sea	August 2010 to July 2012, continuous	Nine drifters every 35 days	288

and a weaker, eddy-dominated flow is established in the northern SCS (Figure 5d). Tracks of drifters deployed in the SCS in spring through summer have shown how parcels tend to exit the SCS through Luzon Strait and Taiwan Strait (Centurioni et al., 2007). The flow through Taiwan Strait reverses, and a swift northeastward coastal current flows along the western coast of Taiwan. West of Luzon, the southernmost latitude at which the surface expression of the Kuroshio appears as an organized flow shifts northward from the summer latitude of $\sim 15^{\circ}\text{N}$, near

the southern coast of Lamon Bay, to $\sim 16.5^{\circ}\text{N}$ during the winter monsoon. Concurrently, the northward expression of the NEC slows down.

The square root of the ratio of an eddy to the mean kinetic energy is computed from the drifter velocity data (Figure 5) and used to illustrate the seasonality of the mesoscale variability around Taiwan. During the northeast monsoon season, the Kuroshio, the strong Vietnam current, and the current along the rim of the northern SCS are steady relative to the flow associated with the mesoscale eddies, while eddies dominate the

circulation at the center of the northern SCS and the Pacific subtropical gyre. From April to September, the entire northern SCS circulation becomes eddy dominated, and the eddylike flow of the Pacific subtropical gyre extends more southward ($\sim 13.5^{\circ}\text{N}$) compared to the October to March period, thus justifying the reduced mean speed of the northern NEC observed in the drifter data and the disappearance of the westward surface current between 18°N and 20°N east of Luzon Strait.

Observational evidence supports the concept that the westward-propagating

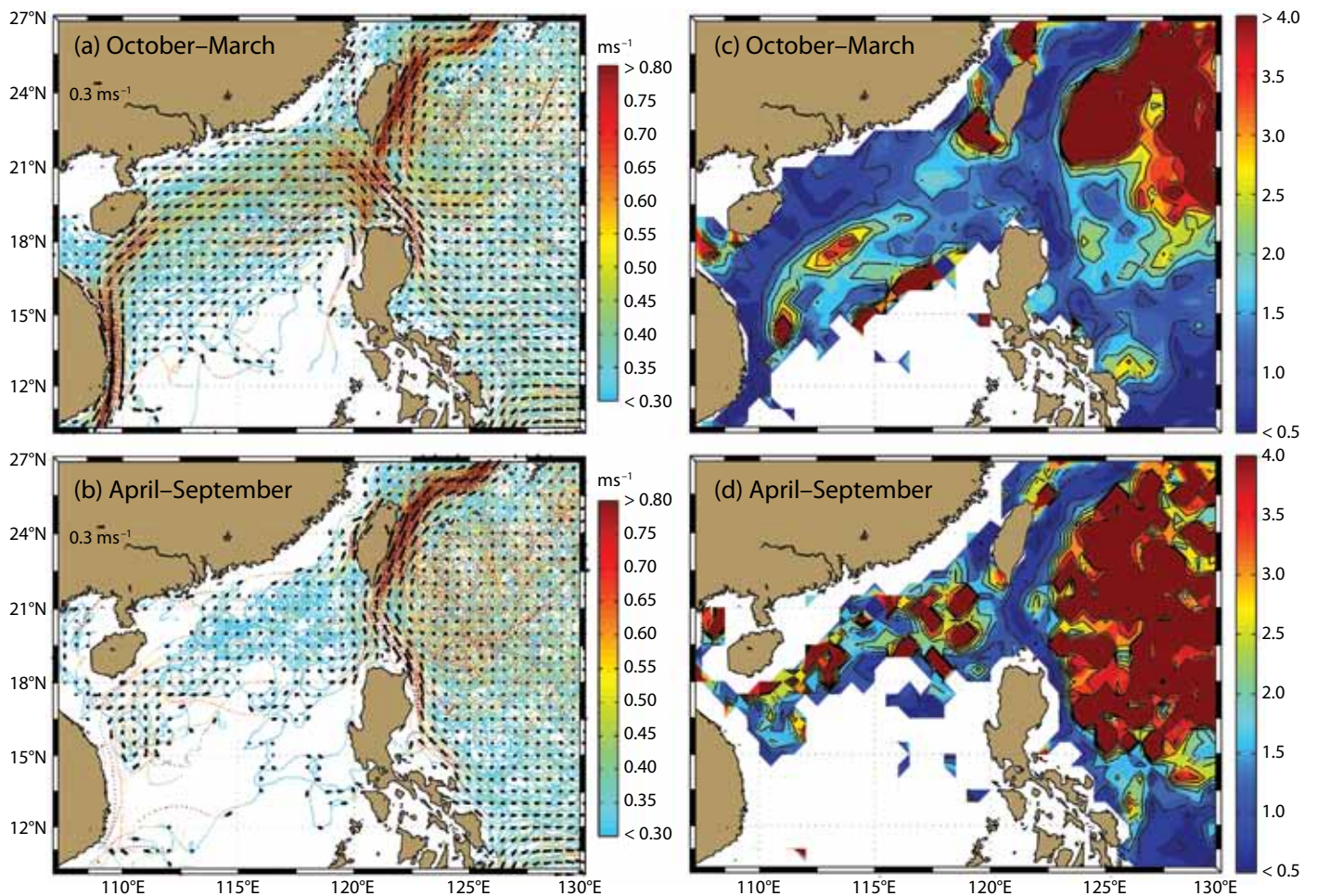


Figure 5. Locations of drifters color-coded in accordance with their six-hourly instantaneous speed overlaid with bin-averaged drifter velocity data for: (a) October through March and (b) April through September. The square root of the ratio of the mean eddy kinetic energy to the mean kinetic energy is computed from six-hourly drifter velocity observations for (c) October through March and (d) April through September. Velocities and ratios were averaged in $0.5^{\circ} \times 0.5^{\circ}$ wide bins and are shown only for bins with more than 15 six-hourly observations.

eddies that reach Taiwan and the Luzon Strait region within the Pacific subtropical gyre, which are therefore responsible for sea level fluctuations east of Taiwan, are positively correlated with the transport of the Kuroshio through the East Taiwan Channel (between Taiwan and Iriomote, one of the westernmost Ryukyu Islands) and cause, during times of low Kuroshio transport, pronounced meandering (intrusion) of the Kuroshio onto the East China Sea continental shelf (see Gawarkiewicz et al., 2011, in this issue), with a periodicity of approximately 100 days.

OBSERVATIONS FROM UNDERWATER GLIDERS

A program of glider observations was undertaken to quantify mesoscale structure within and offshore of the Kuroshio (Figure 6). In April 2007, the first two gliders were deployed, and the last gliders were recovered in June 2008. Deployments lasted three to four months, and the fleet included as many as four gliders at any one time. The two types of autonomous underwater gliders (Rudnick et al., 2004) used, Spray (Sherman et al., 2001) and Seaglider (Eriksen et al., 2001), profiled as deep as 1,000 m, repeating a cycle from the surface to depth about every six hours and covering 6 km. The resulting speed of 0.25 m s^{-1} was sometimes slower than the depth-average currents in the region, presenting some challenges in piloting. Even with these challenges, the gliders were able to survey the offshore eddy-rich region and cross the Kuroshio in Luzon Strait. Variables measured included pressure, temperature, salinity, and depth-average velocity. Throughout the 15 months of glider observations,

over 5,000 dives were completed, covering a total of more than 20,000 km in over 1,000 glider days.

The operational plan was for gliders to be deployed off the coast of Luzon, then to follow a zigzag route northward toward Taiwan (Figure 6a). Currents tended to be weak in the deployment region, so gliders followed the planned track relatively precisely. Mesoscale currents increased to the north, so gliders could not always follow the same path as 1,000 m-depth-average currents approached or exceeded 0.25 m s^{-1} . Three gliders traveled down the axis of the Kuroshio as it entered the SCS through southern Luzon Strait, finally crossing the current at 20°N .

A crossing of the Kuroshio into the SCS shows the hydrographic structure of the region (Figure 6b). The high-salinity NPTW near 200 m depth is apparent, as is the low-salinity NPIW near 500 m. The inshore edge of the Kuroshio (near 450 km distance) is marked by a front in salinity, indicating penetration of NPTW into the SCS. The magnitude of the NPIW salinity minimum also decreases across the Kuroshio. Surface low-salinity water originates in the SCS. Fluctuations in the depth of isopycnals are reflections of mesoscale processes and internal waves.

The dominant water masses, NPTW and NPIW, are regions of thermohaline fluctuations on isopycnals. This thermohaline variability (Veronis, 1972; Jackett and McDougall, 1985), which by definition does not affect density, has been called “spice” (Munk, 1981). In the section across the Kuroshio (Figure 6b), spice variability can be seen as the changes in salinity (color) along isopycnals (black contours), especially in

the salinity extrema. Variations in spice on a wide range of scales are a consistent feature of the observations.

We examine changes in thermohaline structure along the glider trajectory indicated by the solid black line in Figure 6a. Vertical profiles of potential temperature plotted against salinity (Figure 6c) clearly show the salinity extrema of NPTW and NPIW. These extrema are largest in the south and weaken moving northward following the path of the mean flow. Mixing with surrounding water, either along or across isopycnals, causes this reduction in the salinity extrema, under the traditional assumption that water properties are derived from end members. The mean northward 1,000 m depth average flow along the glider trajectory was 0.10 m s^{-1} , so the water column would take about three months to traverse the region. The changes in the water masses are thus remarkably rapid.

We may gain some insight into the processes causing stirring of NPTW and NPIW through examination of potential temperature on isopycnals (Figure 6d). This rather simple expression of spice demonstrates one of the most robust features in the glider observations. Layers of strong spice variability coincide with the dominant water masses. Apparently, stirring is most obvious along salinity extrema, because these waters are the newest in the sense that they were most recently ventilated. That is, there is a large-scale gradient available to be stirred by the prevalent mesoscale eddies. It is often the case that spice gradients in the two layers align in the vertical because the eddies are thick enough to stir both layers. Between the extrema is a layer of very weak spice variability near 26.5 kg m^{-3} . The same

eddies affect the quiet layer, but the effects are not obvious because there is no large-scale gradient to be stirred. This lack of a large-scale gradient near 15°C is seen in the tightness of the temperature-salinity relationship (Figure 6c).

Isopycnal processes, as manifest in spice variability (Figure 6d), and

diapycnal mixing cause the reduction in salinity extrema (Figure 6c). An open question is the contribution of isopycnal and diapycnal processes to the observed thermohaline modification. Assuming only diapycnal mixing causes the reduction in salinity in the NPTW, an order-of-magnitude calculation of eddy

diffusivity proceeds as follows. Take the reduction in salinity to be 0.1 psu, and the time for this change to occur to be 100 days. The mean vertical curvature of salinity on isopycnals in the NPTW is -1×10^{-4} psu m^{-2} (this can be estimated from Figure 6b,c), so the inferred diffusivity is 1×10^{-4} $m^2 s^{-1}$. This value

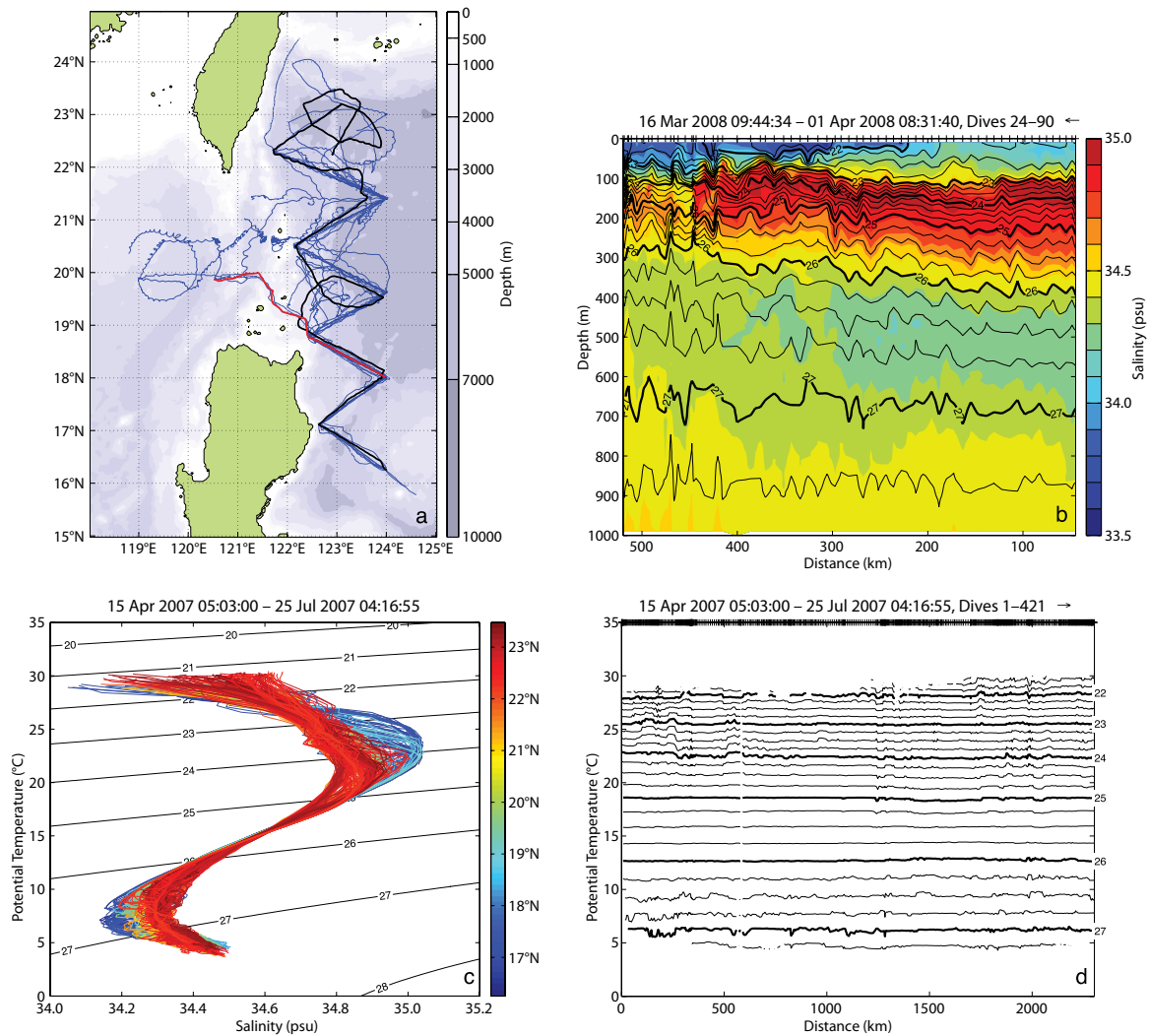


Figure 6. (a) Glider tracks in the region of the Kuroshio from April 2007 through July 2008. Thirteen glider deployments produced over 5,000 dives to as deep as 1,000 m, covering more than 20,000 km in over 1,000 glider-days. (b) A section along the red track in panel (a). Salinity is contoured in color, and potential density is contoured with black lines and an interval of 0.25 kg m^{-3} . Tick marks along the top indicate the locations of profiles. The section follows the Kuroshio as it goes through Luzon Strait from the Pacific, and finally crosses the current into the South China Sea. (c) Profiles of potential temperature against salinity, colored by latitude along the black track in panel (a). Note the spread in salinity in the regions of the salinity extrema. (d) Potential temperature on isopycnals (with a spacing of 0.25 kg m^{-3}) along the black track in panel (a). Tick marks along the top show the locations of profiles. Note the two layers of strong variability corresponding to the salinity extrema in panel (c). Also note the region of weak variability near 15°C.

is an order of magnitude larger than the $1 \times 10^{-5} \text{ m}^2 \text{ s}^{-1}$ canonical value in the upper thermocline from microstructure measurements. Presumably, the horizontal stirring apparent in spice helps to increase the eddy diffusivity averaged over large temporal and spatial scales. The calculation of eddy diffusivity is very rough, with the time required for the NPTW salinity maximum to be eroded particularly worth scrutiny. However, this erosion is certainly occurring, suggesting strong mixing.

The finding of layers of enhanced spice variability is not unique to this region. These layers have also been identified through sustained glider observations in the California Current System (Todd et al., 2011) and in the subtropical gyre north of Hawaii (Cole and Rudnick, 2011). In each case, the high variance spice layers coincide with recently ventilated waters, or with named water masses. This sort of spice variance was previously identified in ship surveys using towed vehicles (i.e., Ferrari and Rudnick, 2000; Hodges and Rudnick, 2006); however, the persistence of these layers was unknown as they were observed through sections occupied only once. With sustained glider observations, it is now becoming clear that layers of persistent spice variance occur throughout the ocean, often coinciding with the intrusion of major water masses.

CONCLUSION

A combination of the historical data record and recent focused observations is establishing the mean state of the Kuroshio near its origins. From humble beginnings at the termination of the NEC off the coast of the Philippines, the Kuroshio grows to a powerful current

leaving the northwest coast of Taiwan. Along the way, the Kuroshio loops into, and back out of, Luzon Strait. A second core of strong flow joins the main Kuroshio from the east offshore of Taiwan, increasing the transport.

Seasonal variability, driven by the monsoon, is a prominent feature of the region. Wind forcing during the strong northeast winter monsoon pushes the core of the Kuroshio closer to the Taiwan coast. Also in winter, the Kuroshio sends a net flow into the SCS, and a strong southward boundary current along the east coast of Vietnam develops. The summer surface flow pattern suggests that near-surface water parcels exit the South China Sea through Luzon Strait to join the Kuroshio.


Mesoscale variability, at timescales shorter than seasonal and longer than a day, dominates flow in the region, especially away from the Kuroshio core. The source of the mesoscale variability is the object of continuing study, but instability in the STCC to the east is certainly a factor. Mesoscale structure is especially apparent in hydrographic sections. The mesoscale stirring manifests itself as interleaving in the dominant water masses, that is, the shallow salty NPTW and the deeper fresh NPIW. The stirring participates in the turbulent cascade, and a back-of-the-envelope calculation suggests enhanced mixing in this region.

An active ONR-sponsored observational and modeling program, “Origins of the Kuroshio and Mindanao Current,” aims to quantify patterns of flow and fluxes with a goal of establishing predictability. At issue is how the NEC feeds the Kuroshio and the Mindanao Current, and what dynamics determine the partitioning into northward and

southward flow. Analyses of large-scale observations, for example, satellite sea surface height, suggest interannual variability in the area of the bifurcation, with a particularly southerly location in recent years. The bifurcation location is predictable from basin-scale models driven by wind stress. In situ observations gathered using surface drifters and profiling floats deployed in the NEC are being used to quantify how the westward flow splits near the bifurcation. Gliders are being deployed off Palau to do repeated sections across the NEC and the Mindanao Current. Gliders launched from Taiwan will cross the Kuroshio off northern Luzon and southern Taiwan. A final glider section in the SCS will document the net transport from the Pacific. Moorings will be placed at the southern end of Luzon Strait to monitor the Kuroshio flow at this critical point. Forward and assimilating models, and objective analyses, are being used in combination with the observations to establish predictability. If these efforts are fully successful, they promise fundamental advances in the understanding of the NEC, the Kuroshio, and the Mindanao Current.

ACKNOWLEDGEMENTS

We are grateful to the Office of Naval Research, whose support has been essential to many of the observational programs reported here. We acknowledge funding through ONR grants N00014-06-1-0776 (DLR), N00014-10-1-0273 (DLR and LC), N00014-03-1-0474 (LC), N00014-08-1-0557 (LC), N00014-10-1-0397 (RCL), N00014-06-1-0751, and N00014-10-1-0311 (CML), and NOAA Global Drifter Program grant NA17RJ1231 (LC). The Ocean

Data Bank of Taiwan's National Science Council provided the historical CTD and shipboard ADCP data. SJ, JW, and CSC are financially supported by the National Science Council under grant NSC98-2611-M-002-019-MY3. Hanjin Shipping Co., Hyundai Merchant Marine, and the Coast Guard of Taiwan are gratefully acknowledged for deploying most of the Northwest Pacific drifter array. The Instrument Development Group at Scripps Institution of Oceanography was largely responsible for the success of the Spray glider operations. 

REFERENCES

- Centurioni, L.R., P.P. Niiler, Y.Y. Kim, V.A. Sheremet, and D.K. Lee. 2007. Near surface dispersion of particles in the South China Sea. Pp. 73–75 in *Lagrangian Analysis and Prediction of Coastal and Ocean Dynamics*. A.D.K.A. Griffa, A.J. Mariano, T. Özgökmen, and T. Rossby, eds, Cambridge University Press.
- Centurioni, L.R., P.P. Niiler, and D.K. Lee. 2004. Observations of inflow of Philippine Sea surface water into the South China Sea through the Luzon Strait. *Journal of Physical Oceanography* 34:113–121, [http://dx.doi.org/10.1175/1520-0485\(2004\)034<0113:OOIOPS>2.0.CO;2](http://dx.doi.org/10.1175/1520-0485(2004)034<0113:OOIOPS>2.0.CO;2).
- Centurioni, L.R., P.N. Niiler, and D.K. Lee. 2009. Near-surface circulation in the South China Sea during the winter monsoon. *Geophysical Research Letters* 36, L06605, <http://dx.doi.org/10.1029/2008gl037076>.
- Cole, S.T., and D.L. Rudnick. In press. The spatial distribution and annual cycle of upper ocean thermohaline structure. *Journal of Geophysical Research*.
- Eriksen, C.C., T.J. Osse, R.D. Light, T. Wen, T.W. Lehman, P.L. Sabin, J.W. Ballard, and A.M. Chiodi. 2001. Seaglider: A long-range autonomous underwater vehicle for oceanographic research. *IEEE Journal of Oceanic Engineering* 26:424–436, <http://dx.doi.org/10.1109/48.972073>.
- Ferrari, R., and D.L. Rudnick. 2000. Thermohaline variability in the upper ocean. *Journal of Geophysical Research* 105:16,857–16,883, <http://dx.doi.org/10.1029/2000JC900057>.
- Fine, R.A., R. Lukas, F.M. Bingham, M.J. Warner, and R.H. Gammon. 1994. The western Equatorial Pacific: A water mass crossroads. *Journal of Geophysical Research* 99:25,063–25,080, <http://dx.doi.org/10.1029/94JC02277>.
- Gawarkiewicz, G., S. Jan, P.F.J. Lermusiaux, J.L. McClean, L. Centurioni, K. Taylor, B. Cornuelle, T.F. Duda, J. Wang, Y.J. Yang, and others. 2011. Circulation and intrusions northeast of Taiwan: Chasing and predicting uncertainty in the cold dome. *Oceanography* 24(4):110–121, <http://dx.doi.org/10.5670/oceanog.2011.99>.
- Hodges, B.A., and D.L. Rudnick. 2006. Horizontal variability in chlorophyll fluorescence and potential temperature. *Deep-Sea Research Part I* 53:1,460–1,482, <http://dx.doi.org/10.1016/j.dsr.2006.06.006>.
- Hu, C.-K., C.-T. Chiu, S.-H. Chen, J.-Y. Kuo, S. Jan, and Y.-H. Tseng. 2010. Numerical simulation of barotropic tides around Taiwan. *Terrestrial Atmospheric and Oceanic Sciences* 21:71–84, [http://dx.doi.org/10.3319/TAO.2009.05.25.02\(IWNOP\)](http://dx.doi.org/10.3319/TAO.2009.05.25.02(IWNOP)).
- Jackett, D.R., and T.J. McDougall. 1985. An oceanographic variable for the characterization of intrusions and water masses. *Deep-Sea Research* 32:1,195–1,207, [http://dx.doi.org/10.1016/0198-0149\(85\)90003-2](http://dx.doi.org/10.1016/0198-0149(85)90003-2).
- Jan, S., D.D. Sheu, and H.M. Kuo. 2006. Water mass and throughflow transport variability in the Taiwan Strait. *Journal of Geophysical Research* 111, C12012, <http://dx.doi.org/10.1029/2006jc003656>.
- Jan, S., J. Wang, C.-S. Chern, and S.-Y. Chao. 2002. Seasonal variation of the circulation in the Taiwan Strait. *Journal of Marine Systems* 35:249–268, [http://dx.doi.org/10.1016/S0924-7963\(02\)00130-6](http://dx.doi.org/10.1016/S0924-7963(02)00130-6).
- Johns, W.E., T.N. Lee, D.X. Zhang, R. Zantopp, C.T. Liu, and Y. Yang. 2001. The Kuroshio east of Taiwan: Moored transport observations from the WOCE PCM-1 array. *Journal of Physical Oceanography* 31:1,031–1,053, [http://dx.doi.org/10.1175/1520-0485\(2001\)031<1031:TKEOTM>2.0.CO;2](http://dx.doi.org/10.1175/1520-0485(2001)031<1031:TKEOTM>2.0.CO;2).
- Liang, W.D., T.Y. Tang, Y.J. Yang, M.T. Ko, and W.S. Chuang. 2003. Upper-ocean currents around Taiwan. *Deep-Sea Research Part I* 50:1,085–1,105, [http://dx.doi.org/10.1016/S0967-0645\(03\)00011-0](http://dx.doi.org/10.1016/S0967-0645(03)00011-0).
- Liu, C.S., S.Y. Liu, S.E. Lallemand, N. Lundberg, and D.L. Reed. 1998. Digital elevation model offshore Taiwan and its tectonic implications. *Terrestrial Atmospheric and Oceanic Sciences* 9:705–738.
- Munk, W. 1981. Internal waves and small-scale processes. Pp. 264–291 in *Evolution of Physical Oceanography*. B.A. Warren and C. Wunsch, eds, The MIT Press, Cambridge, MA.
- Niiler, P.P. 2001. The world ocean surface circulation. Pp. 193–204 in *Ocean Circulation and Climate: Observing and Modelling the Global Ocean*. G. Siedler, J. Church, and J. Gould, eds, Academic Press.
- Qiu, B., and S.M. Chen. 2010. Interannual variability of the North Pacific Subtropical Countercurrent and its associated meso-scale eddy field. *Journal of Physical Oceanography* 40:213–225, <http://dx.doi.org/10.1175/2009jpo4285.1>.
- Rudnick, D.L., R.E. Davis, C.C. Eriksen, D.M. Fratantoni, and M.J. Perry. 2004. Underwater gliders for ocean research. *Marine Technology Society Journal* 38:73–84, <http://dx.doi.org/10.4031/002533204787522703>.
- Sherman, J., R.E. Davis, W.B. Owens, and J. Valdes. 2001. The autonomous underwater glider "Spray." *IEEE Journal of Oceanic Engineering* 26:437–446, <http://dx.doi.org/10.1109/48.972076>.
- Todd, R.E., D.L. Rudnick, M.R. Mazloff, B.D. Cornuelle, and R.E. Davis. In press. Thermohaline structure in the California Current System: Observations and modeling of spice variance. *Journal of Geophysical Research*.
- Veronis, G. 1972. On properties of seawater defined by temperature, salinity, and pressure. *Journal of Marine Research* 30:227–255.